Environmental Science & Technology

ARTICLE

pubs.acs.org/est

More than the Ions: The Effects of Silver Nanoparticles on *Lolium multiflorum*

Liyan Yin,[†,‡,§] Yingwen Cheng,[‡,⊥] Benjamin Espinasse,[‡,¶] Benjamin P. Colman,[‡,§] Melanie Auffan,[#] Mark Wiesner,[‡,¶] Jerome Rose,[‡,#] Jie Liu,[‡,⊥] and Emily S. Bernhardt*[,‡,§]

[†]Key Laboratory of Aquatic Botany and Watershed Ecology, Wuhan Botanical Garden, Chinese Academy of Sciences, Wuhan, 430074, People's Republic of China

[‡]Center for the Environmental Implications of Nanotechnology, [§]Department of Biology, [⊥]Department of Chemistry, and [¶]Department of Civil and Environmental Engineering, Duke University, Durham, North Carolina 27708, United States

[#]CEREGE UMR 6635 CNRS/Aix-Marseille University, iCEINT International Consortium for the Environmental Implications of NanoTechnology, 13545 Aix-en-Provence, France

Supporting Information

ABSTRACT: Silver nanoparticles (AgNPs) are increasingly used as antimicrobial additives in consumer products and may have adverse impacts on organisms when they inadvertently enter ecosystems. This study investigated the uptake and toxicity of AgNPs to the common grass, *Lolium multiflorum*. We found that root and shoot Ag content increased with increasing AgNP exposures. AgNPs inhibited seedling growth. While exposed to 40 mg L^{-1} GA-coated AgNPs, seedlings failed to develop root hairs, had highly vacuolated and collapsed cortical cells and broken epidermis and rootcap. In contrast, seedlings exposed to identical concentrations of $AgNO_3$ or supernatants of ultracentrifuged AgNP solutions showed no such abnormalities. AgNP toxicity was influenced by total NP surface area with smaller AgNPs (6 nm) more strongly affecting growth than did similar concentrations of larger (25 nm) NPs for a given mass. Cysteine (which binds Ag^+) mitigated the effects of $AgNO_3$ but did not reduce the toxicity of AgNP treatments. X-ray spectro-microscopy documented silver speciation within exposed roots and suggested that silver is oxidized within plant tissues. Collectively, this study suggests that growth inhibition and cell damage can be directly attributed either to the nanoparticles themselves or to the ability of AgNPs to deliver dissolved Ag to critical biotic receptors.

INTRODUCTION

Engineered nanoparticles (ENPs) are defined as intentionally produced particles which (a) have a characteristic dimension between 1 and 100 nm and (b) possess novel properties that are not shared by non-nanoscale particles with the same chemical composition.[1] Silver nanoparticles (AgNPs) are increasingly used for their antimicrobial properties in detergents, plastics, and textiles.[2,3] Silver is one of the most toxic trace metals known,[4] though the mechanisms of AgNP toxicity have not been fully elucidated. In particular, there is debate as to whether toxicity is specifically related to nanoparticles or is due to the effects of dissolved forms of Ag released from ENPs. It is reported that ionic silver (Ag^+) released from AgNPs inhibits respiratory enzymes and induces oxidative stress through generation of reactive oxygen species (ROS).[5] AgNPs were found to reduce cell growth, photosynthesis, and chlorophyll production of a marine diatom (*Thalassiosira weissflogii*), and these toxic effects were from the release of dissolved silver.[6] Similarly, Navarro et al. showed that toxicity of AgNPs to the photosystem II quantum yield of a freshwater alga (*Chlamydomonas reinhardtii*) also depended on the release of Ag^+, perhaps locally at the algal/AgNP interface.[7] However, Choi reported that AgNPs less than 5 nm were more toxic to nitrifying bacteria than larger AgNPs or dissolved Ag, at similar mass concentrations, suggesting toxicity was not solely due to the presence of dissolved silver.[8]

While toxicological studies of AgNPs are increasing, most studies to date have been conducted on bacteria,[8−10] animal and human cells,[5,11] algae,[6,7] and fish.[12] To date, there have been very few studies of the organismal level impact of AgNPs on higher plants.[13,14] Studies on the toxicity of other nanomaterials (TiO_2, ZnO, Mg, Al, Pd, Cu, Si, C60 fullerenes, and multiwall carbon nanotubes) on higher plants show both negative and positive effects on growth (Supporting Information, Table S1).[15,16] In this study, we sought to examine whether AgNPs can be taken up by plant roots and transported to shoots; whether AgNPs are toxic to plants; whether AgNP toxicity could be attributed to nanoparticles or to dissolved silver released from AgNPs; and the extent to which different AgNP sizes affect their toxicity. *Lolium multiflorum* was chosen for use in these experiments for two reasons: it has a fast growth rate, and it is commonly used as model organism in phytotoxicity studies.

MATERIALS AND METHODS

Characterization of AgNPs. Both 6 and 25 nm gum arabic (GA) coated Ag NPs were used in our experiment (see

Received: April 29, 2010
Accepted: January 19, 2011
Revised: January 15, 2011
Published: February 22, 2011

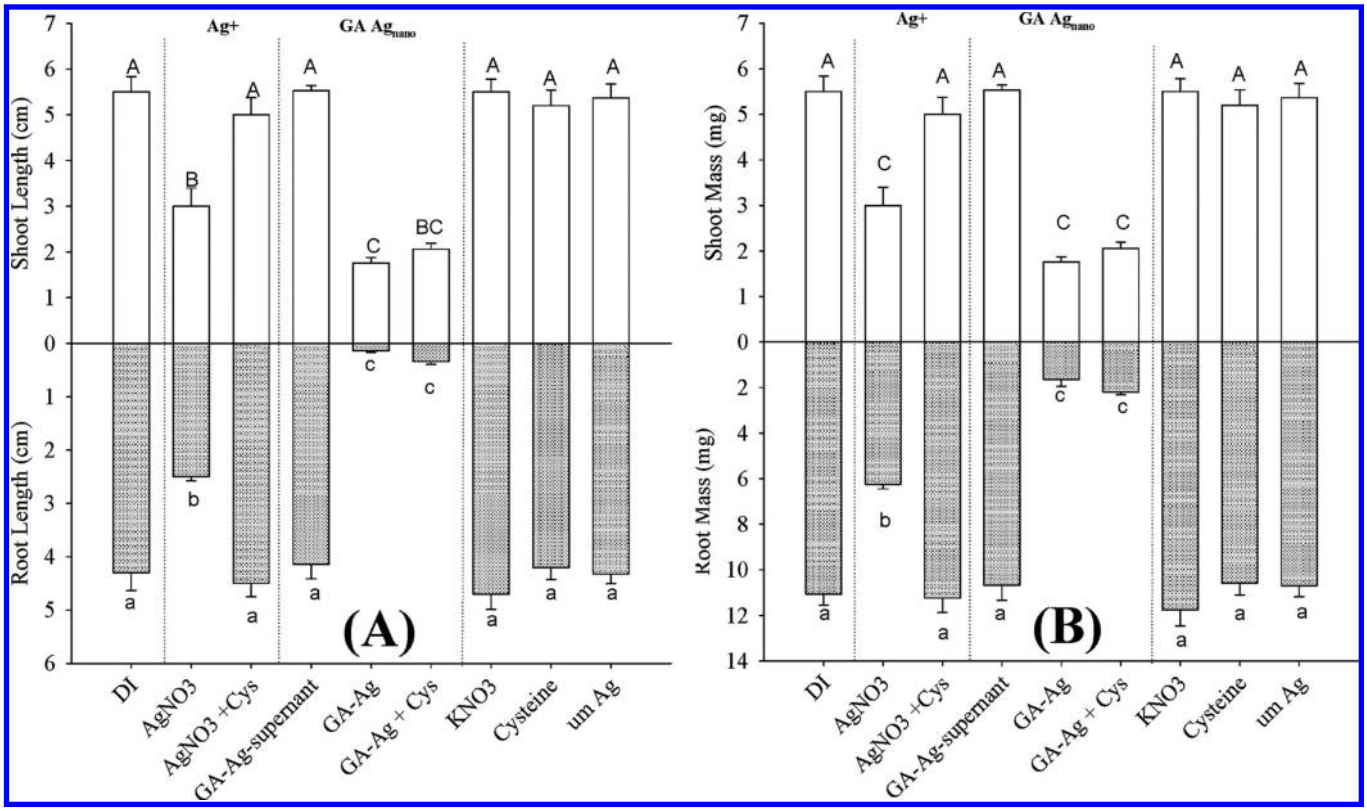

Figure 1. Effect of 40 mg L^{-1}, 6 nm AgNPs and ionic silver on the seedling length (A) and dry weight (B) of *L. multiflorum* after 5 days of exposure. Different letters show significant differences ($p < 0.05$).

Supporting Information for AgNP suspension preparation). The morphology and size were determined using a Tecnai G^2 Twin transmission electron microscope (TEM; FEI, Hillsboro, USA) at 200 kV. UV−vis absorption spectra were acquired using a Cary 500 scan spectrophotometer (Varian, Walnut Creek, USA). Hydrodynamic diameters were obtained by dynamic light scattering (DLS) using a CGS 3-ALV (angle: 90° angle, λ = 632.8 nm). Electrophoretic mobility was measured using a Zetasizer Nano ZS (Malvern, Worcestshire, UK). Zeta potentials were calculated using the Henry equation. Powder X-ray diffraction (XRD) was done using an X'Pert PRO MRD HR diffractometer (PANalytical, Westborough, USA) with a Cu Kα source at 5 kV and 40 mA. To identify the elemental composition on nanoparticle surfaces, an Axis UltraXPS (Kratos, Chestnut Ridge, USA) was used with an aluminum monochromatic energy source. The concentration of AgNPs was determined by an inductively coupled plasma-optical emission spectrometer (ICP-OES; Prism ICP High Dispersion, Teledyne Leeman Laboratories, Hudson, USA) after digestion with 5% HNO_3 for at least 24 h.

The concentration of Ag in supernatants was measured by flame atomic absorption spectroscopy (F-AAS; Perkin-Elmer, Waltham, USA). To ensure that supernatatant Ag was from dissolved silver, we used Amicon Ultra 4 3 kDa centrifugal ultrafiltration units (Millipore, Billerica, USA), which allow dissolved silver to pass but retain AgNPs.[17] Stock suspensions of 250 mg/L were loaded into each filter tube. Tubes were then centrifuged for 20 min, 2000*g*, and the filtrate was digested in 5% HNO_3 for at least 24 h and analyzed by F-AAS.

Plant Culture and Treatment. For each treatment, ∼200 seeds of *L. multiflorum* were soaked in 5 mL test solutions or suspension for 1 h. For each of five replicates per treatment, a filter paper was put into a 100 × 15 mm sterilized Petri dish, and 4 mL of the test solution or suspension was added. A total of 35 seeds were transferred onto each filter paper, and Petri dishes were closed, sealed with tape, and placed in a greenhouse. Temperatures were 25−30 °C in the daytime (16 h) and 15−20 °C at night (8 h).

We tested the dose−response effects of 6 nm GA-coated AgNPs (0, 1, 5, 10, 20, and 40 mg Ag L^{-1}) on *L. multiflorum* growth. We compared shoot elongation, root elongation, and tissue Ag concentration between plants treated with 6 nm GA-coated AgNPs, 25 nm GA-coated AgNPs, 5 μm uncoated silver, and $AgNO_3$ (at 40 mg Ag L^{-1}). Each Ag treatment was added alone and in combination with an excess of the silver binding amino-acid cysteine (45 mg cysteine L^{-1}; L-cysteine, Sigma-Aldrich, St. Louis, USA) to a set of replicates for all three forms of silver. We examined the effects of coatings and other solutes by exposing additional replicates to 5.2 mg NO_3^- N L^{-1} (equivalent to NO_3−N in $AgNO_3$ treatment); to 1 mg L^{-1} GA (equivalent to GA contained within AgNP treatments); and to ionic silver or chemical residues (e.g., boron, citrate) within AgNP supernatants. These supernatant treatments were prepared by ultracentrifugation (197 568*g* for 2 h) of 40 mg L^{-1}, 6 and 25 nm AgNP suspensions.

Biomass and Ag Content Determination. At the end of the exposure, seedlings were washed with flowing tap water for 1 min and then rinsed with 400 mL of deionized water three times. Shoots and roots were separated, and length was measured with calipers, while biomass was measured after drying at 70 °C for 48 h. Ag contents in the shoots and roots were measured by ICP-OES after HNO_3/HCl digestion of plant tissues.

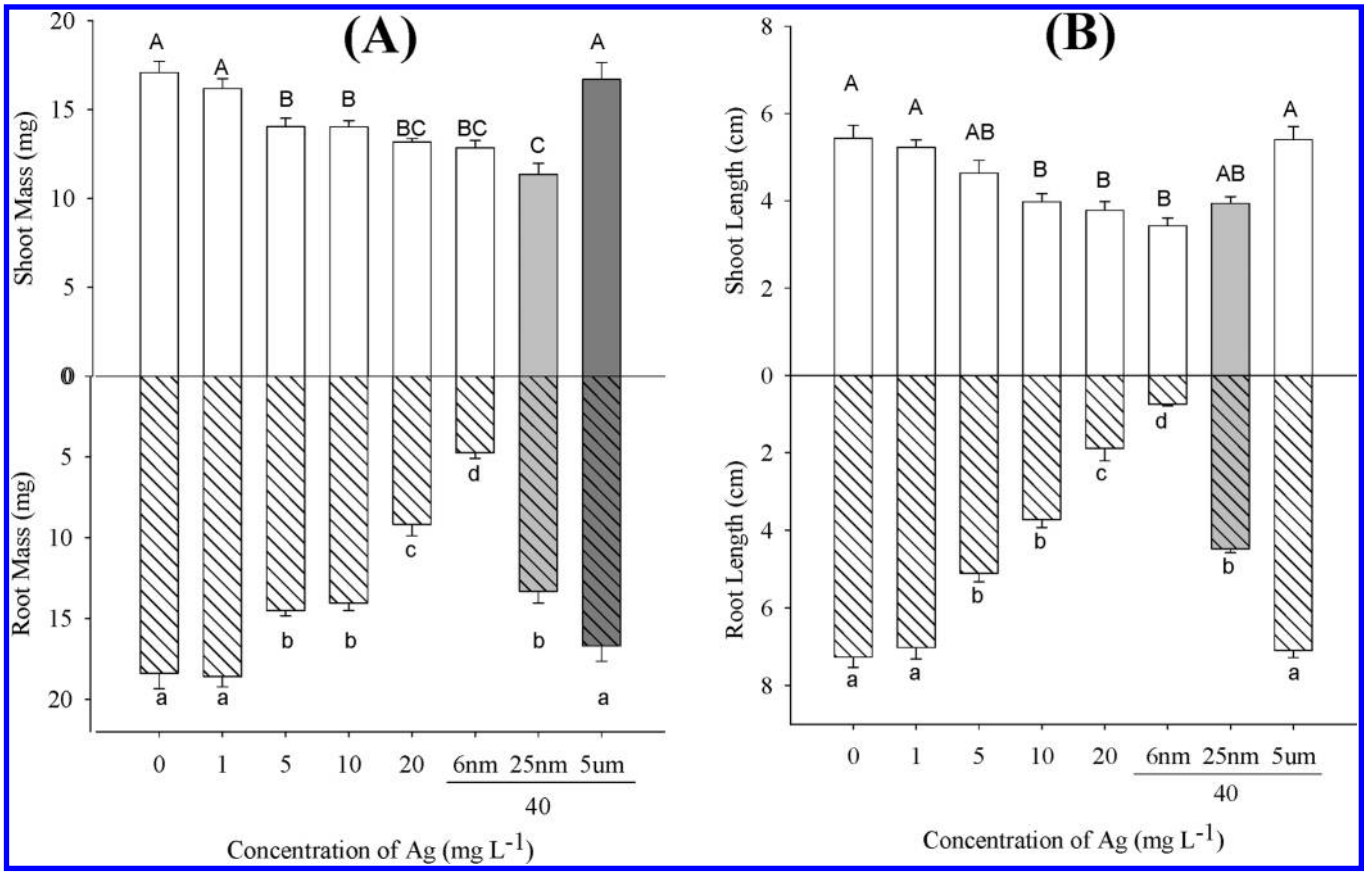

Figure 2. Concentration and size dependent effect of GA-coated AgNPs on the seedling length (A) and biomass (B) of *L. multiflorum* after 7 days of exposure. Different letters show significant differences ($p < 0.05$).

Microscopy. Fresh roots from the 6 nm AgNP, $AgNO_3$, and DDI water control treatments (Barnstead E-pure water; Barnstead, Dubuque, USA) were compared using light microscopy (LM) to examine morphology and cell division state of the root tips. TEM was used to examine the association of nanoparticles outside and within roots. Roots from all treatments were thoroughly washed with deionized water, and for each seedling, we examined 2 cm above the primary root tip.

Samples for LM and TEM were prepared following standard procedures.[18] Root samples were prefixed in 2.5% glutaraldehyde, washed in 0.1 M, pH 7.8 phosphate buffer, postfixed in 1% osmium tetrooxide, dehydrated in ethanol, and infiltrated and embedded in Epon 812 resin. The first 1 mm of root tips were longitudinally sliced (500 nm thick) and stained with 0.05% toluidine blue O in 0.5% sodium borate for LM, and the cross sections (65 nm thick) below the root tips were cut for TEM using a microtome with a diamond knife.

Synchrotron X-ray Fluorescence Microscopy. The distribution of silver on the *L. multiforum* roots and its speciation were assessed using micro X-ray fluorescence (μXRF) and micro X-ray absorption near edge structure (μXANES) at the Ag L_3-edge (3351 eV). Measurements were performed on ID21 beamline at European Synchrotron Radiation Facility (ESRF, Grenoble, France) using the scanning X-ray microscope[19] under vacuum, with a Si(111) monochromator and a silicon drift detector. Elemental maps were obtained by scanning the samples with a 3.7 KeV monochromatic beam and a beam size of 0.5 × 1.2 μm. *L. multiforum* roots exposed to 40 mg/L of GA-coated AgNPs were cross-sectioned (55 μm of thickness) using a Leica cryo-microtome and fixed between Ultralene films. The sections analyzed were cut at 50, 300, 800, and 4000 μm from the apex. The μXRF images and the total fluorescence spectra were, respectively, extracted and fitted using the PyMCA software of the Beamline Instrumentation Software Support group of the ESRF.[20] The μXANES data were obtained after performing standard procedures for pre-edge subtraction and normalization using the iFEFFfit software package.[21]

Statistical Analysis. All errors are expressed as standard deviations (SD). Differences between treatments for the different measured variables were tested using one-way ANOVA (SPSS 13.0.1 for Windows), followed by Tukey HSD tests when differences significant at $p < 0.05$ were found.

RESULTS

Characterization of AgNPs. The GA coated AgNPs are spherical crystallite of zerovalent silver, with mean size of 6.0 ± 1.7 and 25 ± 4 nm. The concentration of dissolved silver within the stock suspension is less than 3% weighted. The specific surface area (SSA) was estimated to be about 100 ± 25 m^2/g (6 nm AgNPs) and 24 ± 4 m^2/g (25 nm AgNPs). In the tested suspension, the GA-coated AgNPs are well dispersed with a negative zeta-potential (−49 to −44 mV). At the end of the experiment, there was no measurable change in particle size as determined by TEM. A detailed characterization is available in the Supporting Information.

Characterization of Toxicity. Both the 6 nm AgNPs and ionic silver significantly reduced growth, resulting in shorter

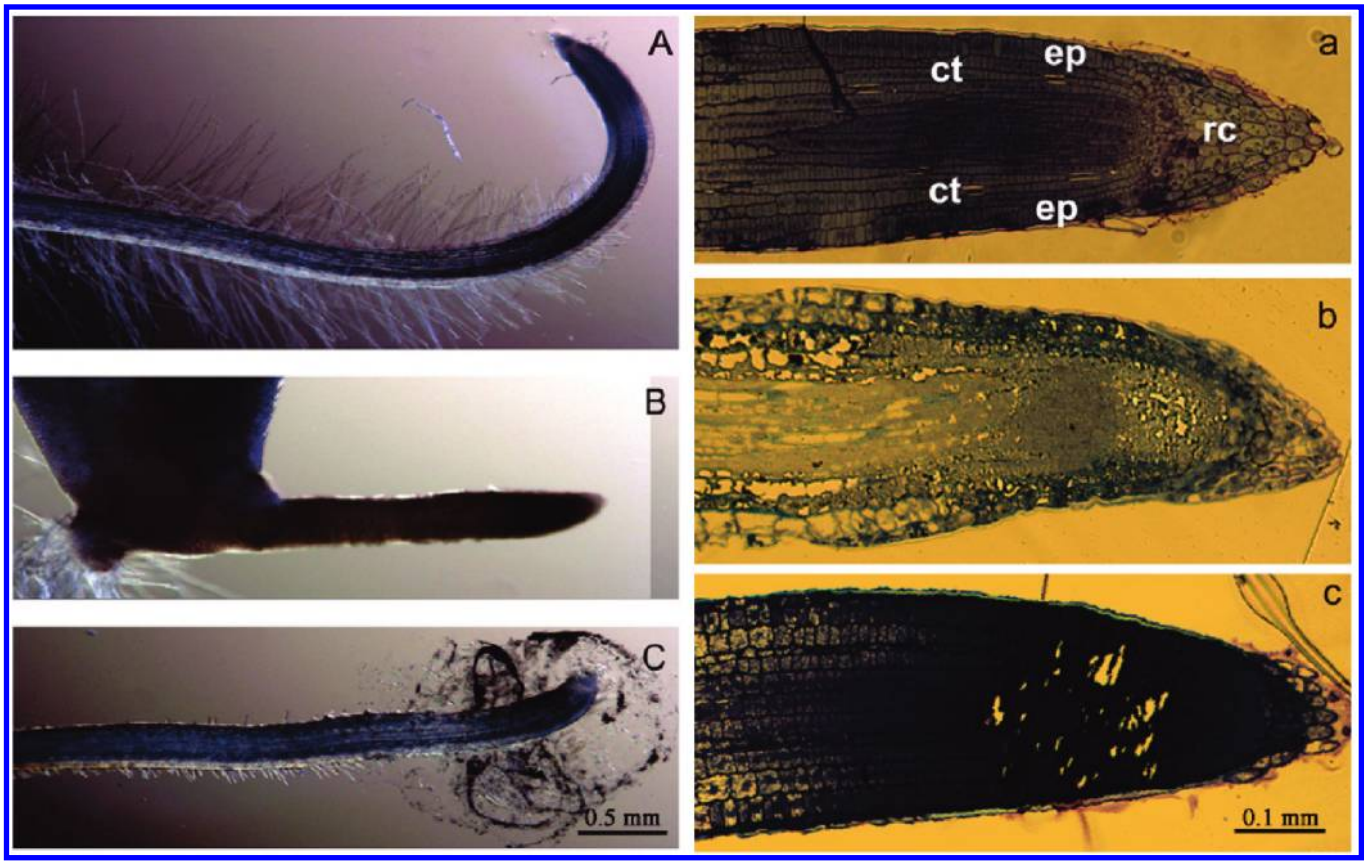

Figure 3. Light microscopic observation of *Lolium multiflorum* root hairs (A−C) and primary root tips (a−c) after 5 days exposure of DDI water control (A and a), 40 mg L^{-1}, 6 nm GA-coated AgNPs (B and b), and 40 mg L^{-1} ionic silver (C and c). rc: rootcap; ep: epidermis; ct: cortex.

shoots and roots and lower biomass (Figures 1 and 2). The growth inhibition from 6 nm AgNPs was significantly stronger than that from $AgNO_3$ at the same total Ag concentration (Figure 1). Cysteine alleviated $AgNO_3$ toxicity for seedling growth but did not significantly alter AgNP toxicity. Supernatants from ultracentrifuged GA-coated AgNPs, as well as controls containing NO_3^-, cysteine, or GA, had no significant toxicity for *L. multiflorum* when compared to the DDI control (Supporting Information, Figures S5 and S6).

As the concentration of 6 nm AgNPs increased from 1 to 40 mg L^{-1}, root biomass decreased from 18.6 ± 1.3 to 4.7 ± 0.7 mg, and root length decreased from 7 ± 0.6 to 0.7 ± 0.08 cm, respectively, showing an increase in toxicity (Figure 2). Roots were more sensitive to AgNPs than were shoots, and their mass decreased by 74.3%, whereas shoots decreased by only 24.6%. Exposure to AgNPs caused both a reduction in root growth rates and the suppression of gravitropic growth (Supporting Information, Figure S7).

Symptoms of the toxicity of 6 nm AgNPs and $AgNO_3$ to *L. multiflorum* were examined through light microscopy of roots, root hairs, and longitudinally sectioned primary root tips. Control roots had long root hairs (Figure 3A), $AgNO_3$ treated roots had shortened root hairs (Figure 3C), and AgNP treated roots had no root hairs (Figure 3B). In control treatments, healthy root tips developed with an intact epidermis, cortex, and vascular cylinder and an intact rootcap at the apex (Figure 3a). In the presence of 40 mg L^{-1} AgNPs, the cortical cells were highly vacuolated and collapsed, and the epidermis and rootcap were also broken (Figure 3b). Cell structures were unaltered in $AgNO_3$ treated roots (Figure 3c).

Localization and Speciation of AgNPs Incubated with Plants. The Ag content of both shoots and roots increased with increasing AgNP exposure (Figure 4A). The bioccumulation factor (BCF; [Ag] in dry plants/[Ag] in treatment solution or suspension) was high for roots with values ranging from 25 to 30 (Figure 4B). Most of this silver appeared to remain associated with the roots, as the translocation factor (TF; [Ag] in shoots/[Ag] in roots) is very low. Light microscopy revealed that many AgNPs adsorbed to the surface of plant roots (Supporting Information, Figure S8) while TEM showed the presence of particulates in AgNP treated roots (Supporting Information, Figure S9). To determine if the roots internalized silver, 55 μm cross sections were analyzed by μXRF (Figure 5). Silver rich areas were found inside the root at 50, 300, 800, and 4000 μm from the apex. In all cases, the total XRF spectra clearly show that the amount of silver is low compared to other major elements in the roots which are also excited at 3.7 KeV (K, P, and S).

The comparison of the silver L_3-edge μXANES spectra of the model compounds (Ag_2O, Ag_2S) and the metallic silver nanoparticles shows that μXANES enables a clear distinction between metallic and oxidized species complexed with S and O/N ligands (Figure 6). All μXANES spectra performed on silver spots observed on μXRF maps (crosses in Figure 5) of root cross sections show similar features that are different from the initial GA-coated AgNPs. The shift of the white line to higher incident energy, the appearance of a distinct absorption edge at 3352 eV (attributed to dipole-allowed $2p_{3/2} \rightarrow 4d$ transitions), and the

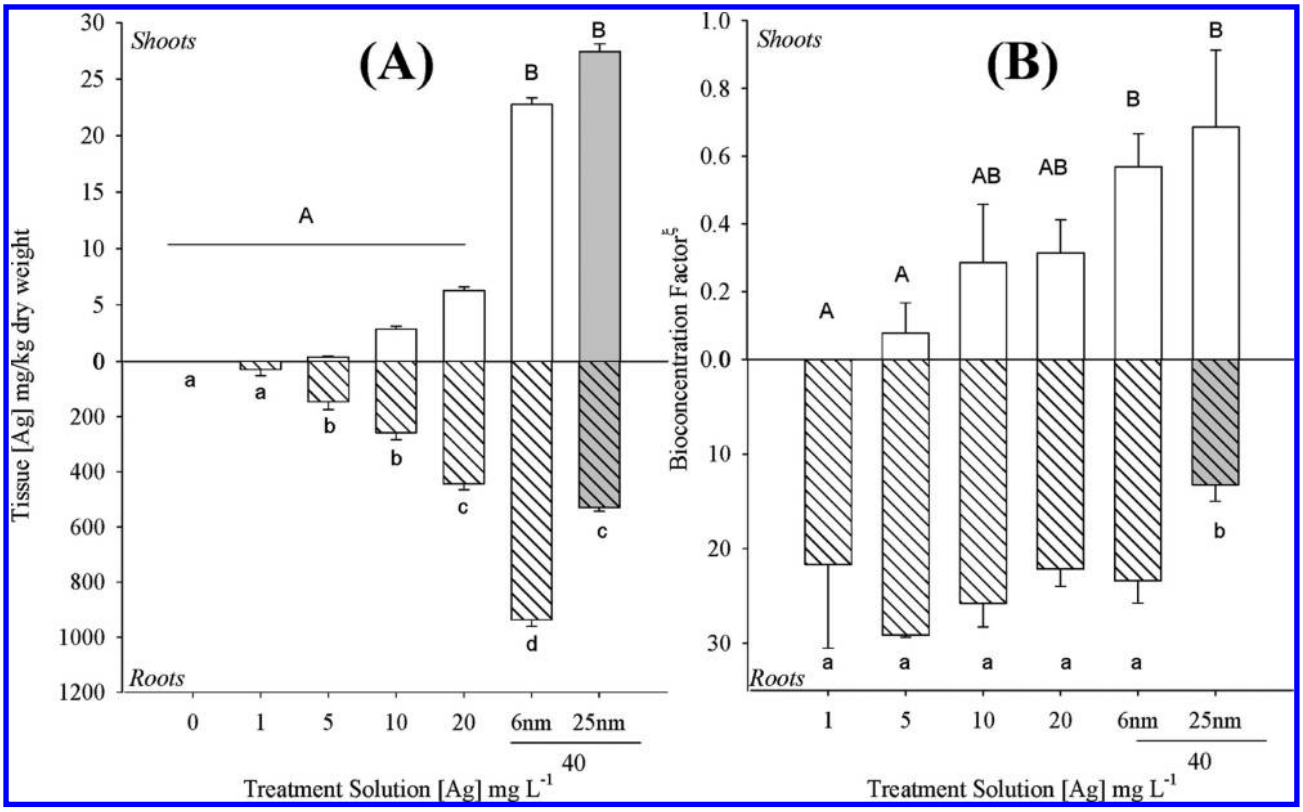

Figure 4. Ag content (A) and bioconcentration factor (B) of silver in the *L. multiflorum* root and shoot after 7 days exposure of 6 nm GA coated AgNPs. ζAg concentration in dry plants/Ag concentration in growth media.

shape of the oscillation between 3555 and 3560 eV are characteristic of the μXANES spectra of oxidized silver species.

DISCUSSION

For the first time, we have differentiated between the phytotoxicity produced by bulk dissolution of AgNPs and possible particle-related effects of AgNPs on the growth of a higher plant, *L. multiflorum*. We find that at similar Ag concentrations AgNPs were more toxic to plants than $AgNO_3$ and that AgNP toxicity led to significant reductions in root growth rate and changes in cell structure and root morphology. Through cysteine binding and supernatant comparisons, we have shown that the toxicity of these GA-coated AgNPs is not just the effect of dissolved Ag released from the NPs. It is important to note that our study represents only a first step in examining plant responses to AgNPs. Here, we examined plant responses at extremely high dosing concentrations (at least 2 orders of magnitude higher than expected concentrations [33]), at a particularly sensitive life history stage (seedling germination), and over very short time scales (5−7 days). While such initial "sledgehammer" experiments are necessary to determine the potential for toxicity, they are insufficient to make predictions about ecosystem impacts of AgNP exposure.[15] Future work must examine whether the toxicity of silver nanoparticles observed in this study occur in this and other plant species under more realistic exposure scenarios, with lower AgNP exposure concentrations, more complex growth conditions (e.g., in soil), and at different life history stages.

Ag Content and Localization in the Plants. AgNPs have been shown to enter bacteria cells,[9] but whether AgNPs can enter plant cells or whether exposure to AgNPs increases plant Ag concentrations is an open question. Silver measured within the roots could result from silver internalization by the roots or adsorption onto the root surface, while silver measured in shoots could result from translocation within the plant or merely from surface adsorption of AgNPs as a result of direct contact with AgNP treatments (as found for CeO_2 exposed plants).[22] Light microscopy revealed that many AgNPs adsorbed to plant roots, and μXRF/μXANES highlighted spots of oxidized silver within root tissues. Two mechanisms of internalization of silver can be proposed: (i) a direct uptake of the AgNPs by the roots followed by the release of oxidized silver species within the root tissues and (ii) a dissolution of the AgNPs on the root surface followed by internalization of the ionic species by the roots. In either case, root exudates or interaction with biofilms surrounding the roots might stimulate oxidative dissolution of AgNPs. In the first hypothesis, the AgNPs could act to bind and insert ionic silver directly into the roots.[7] At present, all available information suggests that AgNPs adsorb to plant root surfaces, that oxidative dissolution leads to the insertion of Ag across the cell membrane, and that once internalized Ag can be translocated between tissues.

Effect of Size on Toxicity of AgNPs. The toxicity of nanoparticles depends on the chemical composition, size, and the shape of particles.[10,23] Smaller Ag nanoparticles with higher surface areas can better interfere with cell membrane function by directly reacting with the membrane and allowing a large number of atoms localized at the surface to interact with cells,[9] as reported for viruses, bacteria, and macrophages.[8,24,25] Our study found that, for a given mass, smaller AgNP particles (6 nm) more strongly affected plant growth than similar concentrations of larger (25 nm) particles. However, when the doses are expressed in units of specific surface area (SSA), the 25 nm AgNPs induce

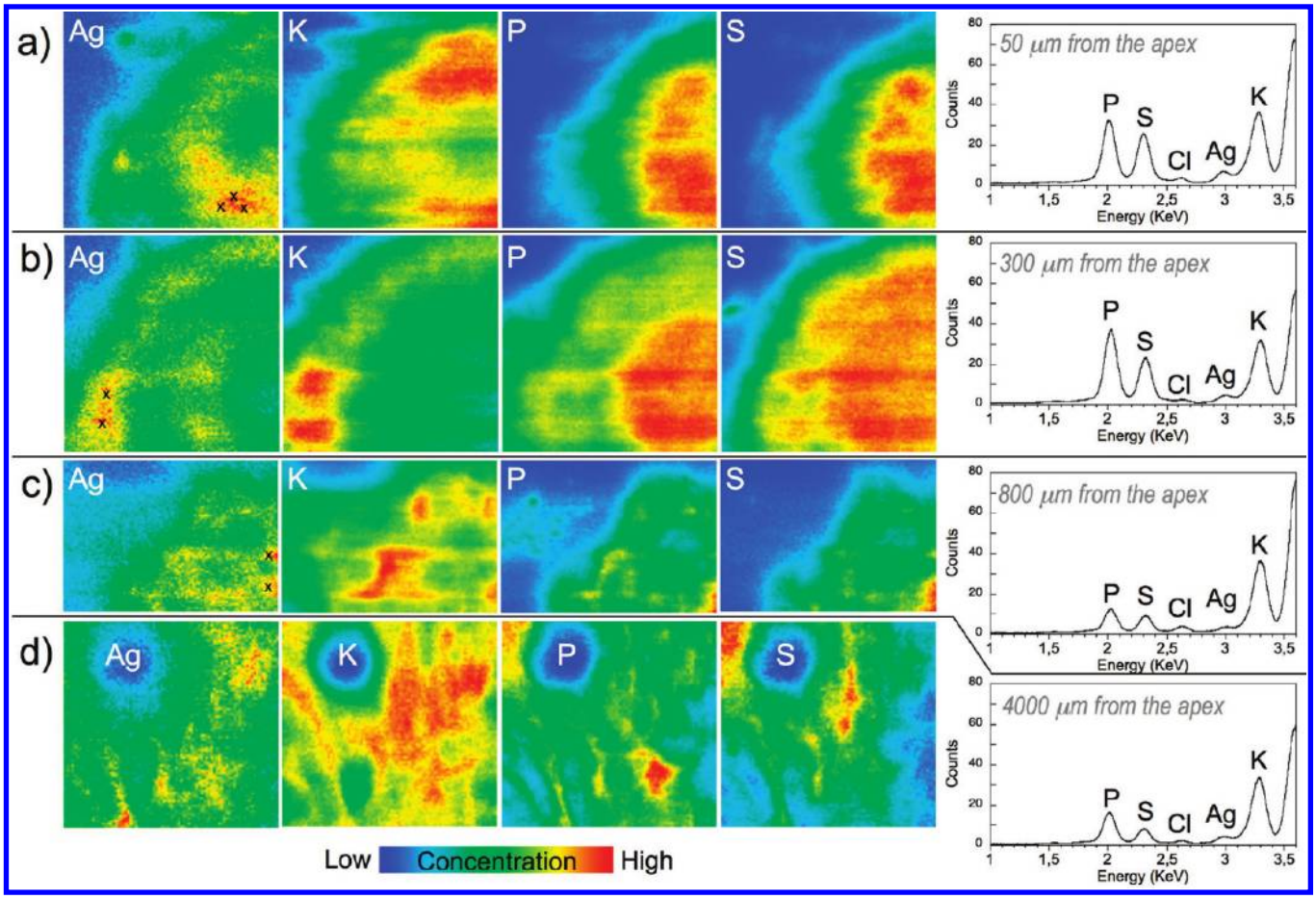

Figure 5. False-color elemental μXRF maps of cross sections of the roots at approximately (a) 50 μm, (b) 300 μm, (c) 800 μm, and (d) 4000 μm from the apex of the roots. Maps (a), (b), and (c) correspond to the bottom left quarter of the root cross-section while maps (d) correspond to the center of the root. The X-ray fluorescence spectra are collected on areas with the highest silver concentration. The crosses are spots where μXANES at the silver L_3-edge were recorded (Figure 6). Incident energy: 3.7 keV; map size: (a) and (b) 100 × 100 μm, (c) 100 × 70 μm, and (d) 85 × 80 μm; step size = 1 μm ; dwell time: 500 ms/pixel.

similar effects to the 6 nm AgNPs. Specifically, when we compare treatments with the same SSA (treatments of 40 mg/L of 25 nm AgNPs and 10 mg/L of 6 nm AgNPs each have 1×10^{-6} m^2/L SSA), the toxicity and the Ag concentrations in roots and shoots were similar (Figure 2).

Particle-Related Effect. Dissolution of metal-based NPs, including silver, copper, nickel, and zinc oxide, and toxicity due to their dissolved forms is one possible mechanism for their toxicity.[6,26,27] Recent studies of AgNPs have frequently attributed their toxicity, at least in part, to the release of dissolved silver.[6,7,10] Our results have shown that cysteine addition effectively quenched the phytotoxicity of $AgNO_3$ but not of AgNPs for *L. multiflorum* and that ionic silver released into suspension from AgNPs (AgNP supernatants) did not lead to altered growth. In these experiments, AgNP toxicity was thus clearly related to zero valent redox state of silver and the nanoparticulate nature of Ag introduced to these systems. The AgNP oxidation (Figure 6) and dissolution within or on biological surfaces may still drive toxicity, but the effect of delivering silver as a particle would be to localize the impact, perhaps to the extent that local biotic receptors might out-compete complexing ligands such as sulfide[28] in the bulk solution.

Mechanisms of Nanoparticle Toxicity. While determining the mechanism of toxicity was beyond the scope of this research, inference can be gained from the observation that root tips bent away from gravity in all silver nanoparticle and $AgNO_3$ treatments. Additionally, in the 40 mg L^{-1} GA-AgNP treatment, the cortical cells were vacuolated and collapsed, and the epidermis and rootcap were also broken. Given that both dissolved silver and AgNPs can provoke the biotic production of reactive oxygen species (ROS)[5,8] and that the resulting oxidative stress can be a mediator of cell apoptosis,[29,30] it is possible that roots were undergoing apoptosis due to silver exposure. Given that root damage could disrupt auxin transport and auxin transport toward the root apex may be required for gravitropism in roots,[31] we speculate that silver induced damage may cause the loss of gravitropism in roots through disruption of auxin transport.

Toxicity of AgNPs May Be Underestimated. In a recently published risk assessment of nanoparticles in the environment, Mueller and Nowack suggested that, ". . .the release of silver in the form of nanoparticles is of subordinate importance compared to the release of ionic Ag from NP".[32] In our study, we found that GA-coated AgNPs were more toxic to *L. multiflorum* than the same concentration of ionic silver. Part of this may be due to higher bioaccumulation for these AgNPs than has been reported for ionic silver species.[4] It may also be that AgNPs can have direct toxic effects without dissolution. Regardless, if the risk of AgNPs to *L. multiflorum* were assessed on the basis of the release of

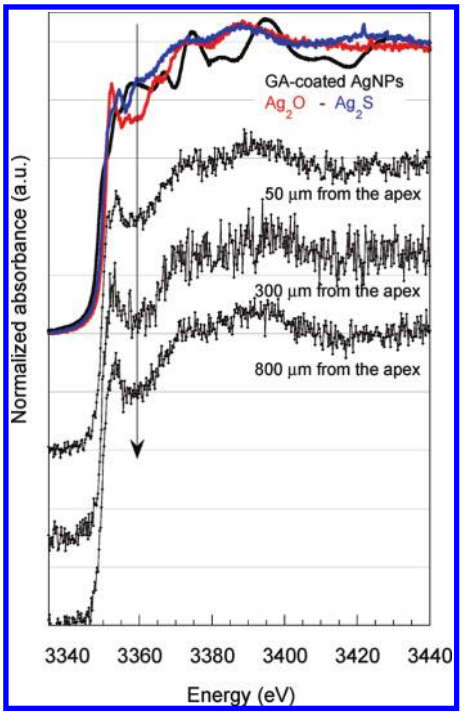

Figure 6. μXANES at the silver L_3-edge of the reference compounds (Ag_2O and Ag_2S), the GA-coated AgNP stock suspension before incubation with the plants, and the silver spots located within the roots (see crosses in Figure 5).

dissolved Ag from GA-AgNPs alone, one would dramatically underestimate the toxic effects.

■ ASSOCIATED CONTENT

Supporting Information. Details of AgNP suspension preparation and AgNP characterization and additional documentation of plant responses to treatments. This material is available free of charge via the Internet at http://pubs.acs.org.

■ AUTHOR INFORMATION

Corresponding Author

*Address: Box 90338, Department of Biology, Duke University, Durham, NC 27708; e-mail: ebernhar@duke.edu; phone: 919.660.7318.

■ ACKNOWLEDGMENT

We thank A. Raju Badireddy for assistance with measurement of Ag content, Cole Matson for assistance in thin sectioning tissue samples, and Cole Matson and Perrine Chaurand for the instrumental role they played in providing us the ability to obtain μXRF/μXANES data. We are grateful to the European Synchrotron Radiation Facility (Grenoble, France) for the provision of beam time and acknowledge ID21 staff (especially Barbara Fayard) for their technical support during data collection. During this work, L.Y. was supported as a visiting scholar at Duke University by a fellowship from the Chinese Academy of Sciences and the National Scientific Foundation of China (30700083). This material is based upon work supported by the National Science Foundation (NSF) and the Environmental Protection Agency (EPA) under NSF Cooperative Agreement EF-0830093, Center for the Environmental Implications of NanoTechnology (CEINT). Any opinions, findings, conclusions, or recommendations expressed in this material are those of the author(s) and do not necessarily reflect the views of the NSF or the EPA. This work has not been subjected to EPA review and no official endorsement should be inferred.

■ REFERENCES

(1) USNTC The National Nanotechnology Initiative: Stragegic Plan. Available at http://www.nano.gov/NNI_Strategic_Plan_2004.pdf; 2004.

(2) Benn, T. M.; Westerhoff, P. Nanoparticle silver released into water from commercially available sock fabrics. *Environ. Sci. Technol.* **2008**, *42* (11), 4133–4139.

(3) Blaser, S. A.; Scheringer, M.; MacLeod, M.; Hungerbuhler, K. Estimation of cumulative aquatic exposure and risk due to silver: Contribution of nano-functionalized plastics and textiles. *Sci. Total Environ.* **2008**, *390* (2−3), 396–409.

(4) Ratte, H. T. Bioaccumulation and toxicity of silver compounds: A review. *Environ. Toxicol. Chem.* **1999**, *18* (1), 89–108.

(5) Kim, S.; Choi, J. E.; Choi, J.; Chung, K. H.; Park, K.; Yi, J.; Ryu, D. Y. Oxidative stress-dependent toxicity of silver nanoparticles in human hepatoma cells. *Toxicol. in Vitro* **2009**, *23* (6), 1076–1084.

(6) Miao, A. J.; Schwehr, K. A.; Xu, C.; Zhang, S. J.; Luo, Z. P.; Quigg, A.; Santschi, P. H. The algal toxicity of silver engineered nanoparticles and detoxification by exopolymeric substances. *Environ. Pollut.* **2009**, *157* (11), 3034–3041.

(7) Navarro, E.; Piccapietra, F.; Wagner, B.; Marconi, F.; Kaegi, R.; Odzak, N.; Sigg, L.; Behra, R. Toxicity of Silver Nanoparticles to Chlamydomonas reinhardtii. *Environ. Sci. Technol.* **2008**, *42* (23), 8959–8964.

(8) Choi, O.; Hu, Z. Q. Size dependent and reactive oxygen species related nanosilver toxicity to nitrifying bacteria. *Environ. Sci. Technol.* **2008**, *42* (12), 4583–4588.

(9) Morones, J. R.; Elechiguerra, J. L.; Camacho, A.; Holt, K.; Kouri, J. B.; Ramirez, J. T.; Yacaman, M. J. The bactericidal effect of silver nanoparticles. *Nanotechnology* **2005**, *16* (10), 2346–2353.

(10) Pal, S.; Tak, Y. K.; Song, J. M. Does the antibacterial activity of silver nanoparticles depend on the shape of the nanoparticle? A study of the gram-negative bacterium Escherichia coli. *Appl. Environ. Microbiol.* **2007**, *73* (6), 1712–1720.

(11) Kim, Y. S.; Kim, J. S.; Cho, H. S.; Rha, D. S.; Kim, J. M.; Park, J. D.; Choi, B. S.; Lim, R.; Chang, H. K.; Chung, Y. H.; Kwon, I. H.; Jeong, J.; Han, B. S.; Yu, I. J. Twenty-eight-day oral toxicity, genotoxicity, and gender-related tissue distribution of silver nanoparticles in Sprague-Dawley rats. *Inhalation Toxicol.* **2008**, *20* (6), 575–583.

(12) Asharani, P. V.; Wu, Y. L.; Gong, Z. Y.; Valiyaveettil, S. Toxicity of silver nanoparticles in zebrafish models. *Nanotechnology* **2008**, *19*, 25.

(13) Kumari, M.; Mukherjee, A.; Chandrasekaran, N. Genotoxicity of silver nanoparticles in Allium cepa. *Sci. Total Environ.* **2009**, *407* (19), 5243–5246.

(14) Stampoulis, D.; Sinha, S. K.; White, J. C. Assay-Dependent Phytotoxicity of Nanoparticles to Plants. *Environ. Sci. Technol.* **2009**, *43* (24), 9473–9479.

(15) Bernhardt, E. S.; Colman, B. P.; Hochella, M.; Cardinale, B.; Nisbet, R.; Richardson, C.; Yin, L. Emerging environmental crisis or part of the Green Revolution: the ecological impacts of nanomaterials in the environment. *J. Environ. Qual.* **2010**, *39*, 1954–1965.

(16) Monica, R. C.; Cremonini, R. Nanoparticles and higher plants. *Caryologia* **2009**, *62* (2), 161–165.

(17) Lok, C. N.; Ho, C. M.; Chen, R.; He, Q. Y.; Yu, W. Y.; Sun, H.; Tam, P. K. H.; Chiu, J. F.; Che, C. M. Silver nanoparticles: partial oxidation and antibacterial activities. *J. Biol. Inorg. Chem.* **2007**, *12* (4), 527–534.

(18) Bozzola, J.; Russell, L. *Electron Microscopy: Principles and Techniques for Biologists*; Jones and Bartlett Publishers: Sudbury, MA, 1992; p 26.

(19) Susini, J.; Salome, M.; Fayard, B.; Ortega, R.; Kaulich, B. The scanning X-ray microprobe at the ESRF "X-ray microscopy" beamline. *Surf. Rev. Lett.* **2008**, *9*, 203–211.

(20) Sole, V. A.; Papillon, E.; Cotte, M.; Walter, P.; Susini, J. A multiplatform code for the analysis of energy-dispersive X-ray fluorescence spectra. *Spectrochim. Acta, Part B* **2007**, *62*, 63–68.

(21) Ravel, B.; Newville, M. ATHENA, ARTEMIS, HEPHAESTUS: data analysis for X-ray absorption spectroscopy using IFEFFIT. *J. Synchrotron Radiat.* **2005**, *12*, 537–541.

(22) Birbaum, K.; Brogioli, R.; Schellenberg, M.; Martinoia, E.; Stark, W. J.; Gunther, D.; Limbach, L. K. No evidence for cerium dioxide nanoparticle translocation in maize plants. *Environ. Sci. Technol.* **2010**, *44* (22), 8718–8723.

(23) Auffan, M.; Rose, J.; Bottero, J. Y.; Lowry, G. V.; Jolivet, J. P.; Wiesner, M. R. Towards a definition of inorganic nanoparticles from an environmental, health and safety perspective. *Nat. Nanotechnol.* **2009**, *4* (10), 634–641.

(24) Carlson, C.; Hussain, S. M.; Schrand, A. M.; Braydich-Stolle, L. K.; Hess, K. L.; Jones, R. L.; Schlager, J. J. Unique cellular interaction of silver nanoparticles: size-dependent generation of reactive oxygen species. *J. Phys. Chem. B* **2008**, *112* (43), 13608–13619.

(25) Elechiguerra, J. L.; Burt, J. L.; Morones, J. R.; Camacho-Bragado, A.; Gao, X.; Lara, H. H.; Yacaman, M. J. Interaction of silver nanoparticles with HIV-1. *J. Nanobiotechnol.* **2005**, *3*, 6.

(26) Griffitt, R. J.; Luo, J.; Gao, J.; Bonzongo, J. C.; Barber, D. S. Effects of particle composition and species on toxicity of metallic nanomaterials in aquatic organisms. *Environ. Toxicol. Chem.* **2008**, *27* (9), 1972–1978.

(27) Limbach, L. K.; Wick, P.; Manser, P.; Grass, R. N.; Bruinink, A.; Stark, W. J. Exposure of engineered nanoparticles to human lung epithelial cells: Influence of chemical composition and catalytic activity on oxidative stress. *Environ. Sci. Technol.* **2007**, *41* (11), 4158–4163.

(28) Kim, B.; Park, C.-S.; Murayama, M.; Hochella, M. F., Jr. Discovery and characterization of silver sulfide nanoparticles in final sewage sludge products. *Environ. Sci. Technol.* **2010**, *44*, 7509–7514.

(29) Chakraborti, T.; Mondal, M.; Roychoudhury, S.; Chakraborti, S. Oxidant, mitochondria and calcium: An overview. *Cell. Signalling* **1999**, *11* (2), 77–85.

(30) Yin, L. Y.; Huang, J. Q.; Li, W.; Liu, Y. D. Microcystin-RR-induced apoptosis in tobacco BY-2 cells. *Toxicon* **2006**, *48*, 204–210.

(31) Dinneny, J. R.; Long, T. A.; Wang, J. Y.; Jung, J. W.; Mace, D.; Pointer, S.; Barron, C.; Brady, S. M.; Schiefelbein, J.; Benfey, P. N. Cell identity mediates the response of Arabidopsis roots to abiotic stress. *Science* **2008**, *320* (5878), 942–945.

(32) Mueller, N. C.; Nowack, B. Exposure modeling of engineered nanoparticles in the environment. *Environ. Sci. Technol.* **2008**, *42* (12), 4447–4453.

(33) Luoma, S. N. *Silver nanotechnologies and the environment: old problems or new challenges*; Woodrow Wilson International Center for Scholars, Project for Emerging Nanotechnol. Available at http://www.pewtrusts.org/uploadedFiles/wwwpewtrustsorg/Reports/Nanotechnologies/Nano_PEN_15_Final.pdf 2008.